Metabolic Imaging of O-linked N-Acetylglucosamine using On-Tissue Hydrolysis and MALDI

Edwin E. Escobar[1], Erin H. Seeley[1], & Jennifer S. Brodbelt[1]
Department of Chemistry[1], The University of Texas at Austin

Overview

- Use of O-GlcNAc hydrolase for *in situ* enzymatic hydrolysis of O-GlcNAc and MS-based imaging of released O-GlcNAc residues from protein in tissue sections.

Introduction

The posttranslational modification, N-linked glycosylation, has been extensively studied in its context to cancer and other diseases, both through traditional proteomics and mass spectrometry imaging.[1,2] However, the attachment of O-linked N-acetylglucosamine (O-GlcNAc) is unique from other common forms of protein glycosylation: (1) it occurs co-translationally within the nucleus of the cell, and (2) it occurs post-translationally in the cytoplasmic compartments.[3] Two enzymes mediate enzymatic installation and removal of O-GlcNAc; O-GlcNAc transferase (OGT) installs the sugar on target proteins, and O-GlcNAc hydrolase (OGA) removes it. The reversible nature of this modification enables it to serve as a nutrient and stress-responsive regulator of diverse cellular processes including epigenetic regulation of gene expression, proteostasis, and stress response.[4] These processes are perturbed during tumorigenesis; thus, variability in O-GlcNAcylation is likely a critical metabolic marker in cancer.[5,6] Here, on-tissue hydrolysis and MALDI imaging are employed to monitor O-GlcNAc rabbit tumor tissue.

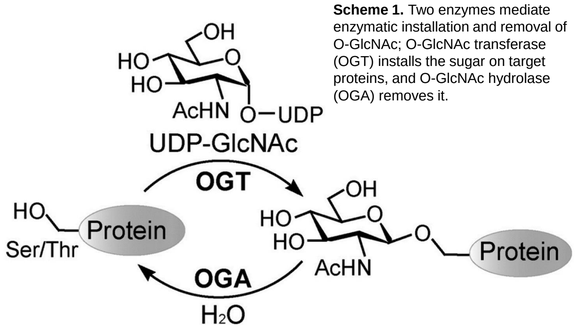

Scheme 1. Two enzymes mediate enzymatic installation and removal of O-GlcNAc; O-GlcNAc transferase (OGT) installs the sugar on target proteins, and O-GlcNAc hydrolase (OGA) removes it.

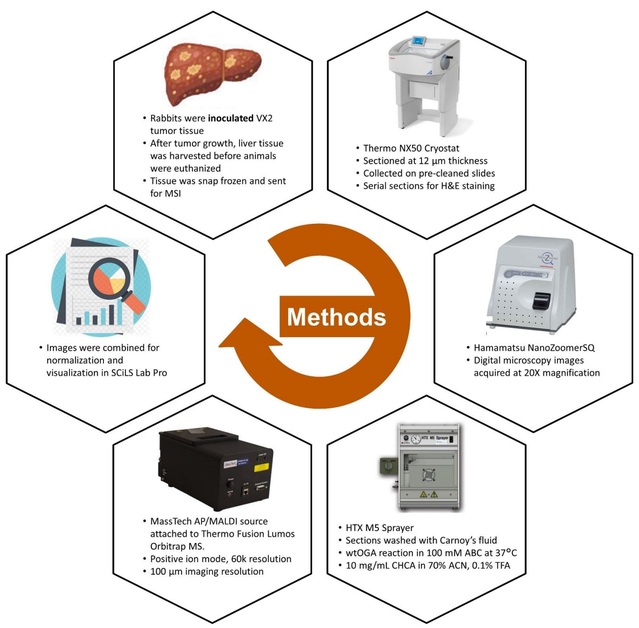

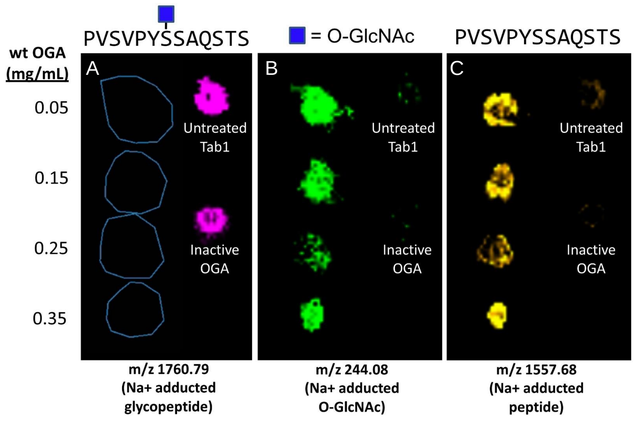

Figure 1. Composite image showing four spots of TAB1 glycopeptide reacted with varying concentrations of wtOGA (left side of each panel). Reactions were compared to two controls, one untreated glycopeptide spot and one treated with an inactive form of OGA (right side of each panel). The sodiated masses of each assessed ion are denoted below each panel. A) shows signal of the intact glycopeptide in the two controls, B) denotes the signal of released O-GlcNAc in the wtOGA reacted spots, and C) shows the signal emanating from deglycosylated TAB1 peptide.

Here, we evaluate the use of MALDI MSI to facilitate the visualization of O-GlcNAc after enzymatic hydrolysis of glycosylated substrates with OGA. O-GlcNAcylation is a critical metabolic marker in cancer and efforts to image O-GlcNAc have revolved around fluorescence based techniques.[4] On-tissue hydrolysis and MALDI imaging are employed to monitor O-GlcNAc in hepatic VX2 tumor tissue from New Zealand White rabbits. In the initial work, we monitor O-GlcNAc released from a standard O-GlcNAc-modified glycopeptide TAB-1 to optimize enzymatic reaction conditions and proper MALDI matrices based on ionization of the released saccharide and deglycosylated peptide. Released O-GlcNAc is observed as a protonated monosaccharide of *m/z* 222.0972, the sodium-cationized monosaccharide of *m/z* 244.0792, or potassium-cationized monosaccharide of m/z 260.0531. The notoriously fragile monosaccharide is also observed as a dehydrated product upon MALDI as the protonated, sodium-cationized, or potassium-cationized oxonium ion, *m/z* 204.0867, 226.0686, or 242.0425, respectively. The detection of O-GlcNAc is most efficient positive ion mode with CHCA matrix compared to DHB.

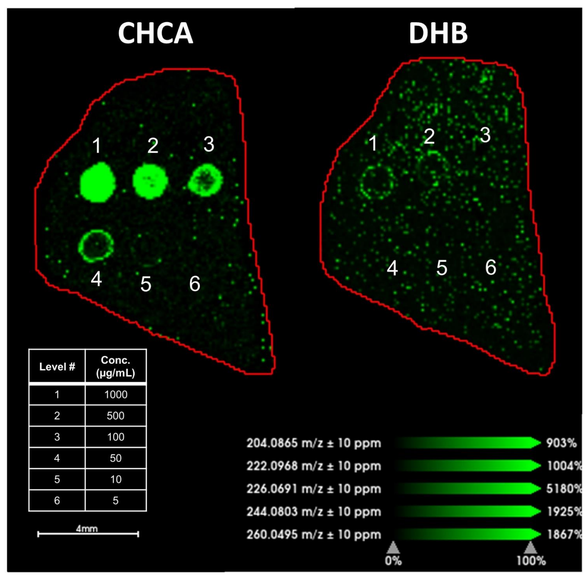

Figure 2. Carnoy's fluid washed tissue sections were spotted with a standard curve of O-GlcNAc at 6 points between 1.0 mg/mL to 5.0 µg/mL. One section was sprayed with CHCA matrix and the other with DHB matrix for MALDI analysis.

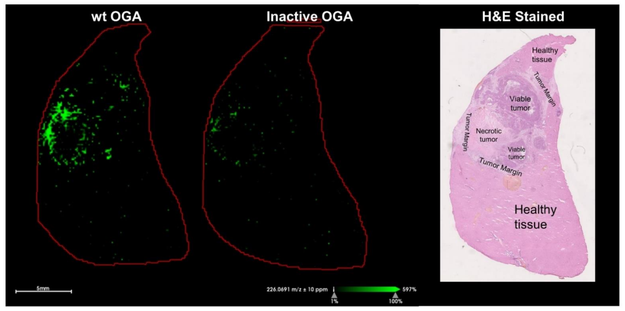

Figure 3. Carnoy's fluid washed tissue sections were treated with wtOGA or inactive OGA, incubated at 37°C, and sprayed with CHCA for MALDI analysis. A serial section was stained with hematoxylin and eosin to visualize pathology of the cells composing the liver section. The sodium-cationized GlcNAc-oxonium m/z 226.0691 – is monitored using SCiLS.

Benchmarks results are shown in Figure 1. TAB1 glycopeptide (0.5 µL of 10 µM solution) was spotted onto a glass slide, sprayed with wtOGA (O-GlcNAcase BT4395 from Bacteroides thetaiotaomicron VPI-5482) and incubated in a humidity chamber at 37° C. O-GlcNAc is released from the peptide and detected by MALDI MSI. As controls, one spot was left untreated with any enzyme, and another was sprayed with an inactive catalytically mutated form of OGA (DT42A mutation). Due to the labile nature of the O-linked GlcNAc modification, low abundances of monosaccharide and deglycosylated peptide are observed for the controls. The monosaccharide is detected on the wtOGA treated areas, and an observed mass shift is seen in the *m/z* of the singly charged TAB1 peptides upon loss of the O-GlcNAc moiety.

In order to determine a lower limit of detection for imaging, a serial dilution of native O-GlcNAc was prepared and spotted on two tissue sections (Figure 2). Given a known volume and concentration of O-GlcNAc standard, instrument acquisition parameters such as pixel size, and the physical tissue thickness, a lower limit of detection can be calculated. Based on a $5.0x10^{-6}$ µg quantity of O-GlcNAc spiked on a 12.0 µm thick section of tissue with a deposited spot diameter of 550 µm, we calculate the limit of detection on tissue to be approximately 420 ng/g.

Initial on-tissue studies show the release of O-GlcNAc after treatment with OGA, with diffuse signal detected in hepatic tumor tissue tumor margins surrounding the viable tumor and necrotic regions (Figure 3). By virtue of the hydrolytic cleavage of O-GlcNAc by OGA, incubation in a humidity chamber is a crucial step in this enzymatical mediated protocol (Figure 4).

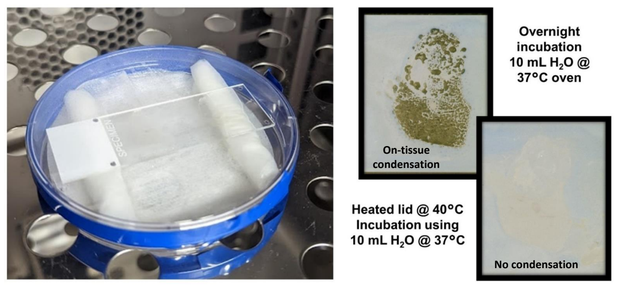

Figure 4. Hydrolysis-based enzymatic protocols require high-humidity for action on tissue. A humidity chamber was constructed using a petri dish and Kimwipes to absorb 10 mL of H_2O. The slide was elevated to protect from wetting and target delocalization. Condensation over the slide was abated by use of a heating pad placed on the lid of the dish, kept at 2-3°C over incubation temperature.

Acknowledgements

RP190617

Erik N.K. Cressman, MD and A. Colleen Crouch, PhD - M.D. Anderson Cancer Center, Houston, TX
David Vocadlo, PhD and Jesus Serrano-Negron – Simon Fraser University, Burnaby, B.C. Canada

After optimization of OGA incubation conditions, MALDI imaging was undertaken on a liver section. Figure 5 illustrates the image obtained based on detection of sodium-cationized O-GlcNAc. O-GlcNAc is localized to both viable tumor and tumor margin regions shown on the H&E-stained liver section. The necrotic tumor region in the center of the stained serial section shows minimal monosaccharide signal, and minimal signal is also observed in the healthy regions of the section. These results are in-line with higher O-GlcNAc levels reported in areas of cellular proliferation and malignancy.

Targeted on-tissue tryptic digestion using SDS-PAGE gel plugs was conducted on regions reporting O-GlcNAc signal.[7] This approach uses an in situ digestion and peptide extraction using polyacrylamide gel permeated with trypsin and use of imaging to direct precise placement onto the tissue section. Peptides were extracted and separated using nanoLC-MS/MS and a HCD-triggered-UVPD approach (2 pulses 1.5 mJ, 193 nm UVPD) for O-GlcNAc localization and analyzed using Protein Metrics Byonic software. In total, 1916 proteins, 14727 unique peptides, and 23 O-GlcNAc modified peptide spectra matches using both HCD/UVPD were traced to the proteins reported in Table 1. While all the proteins reported in Table 1 are reported to be implicated in cancer, calnexin, a ER chaperon protein, is significantly up-regulated in several tumor phenotypes and thus used as a sero-diagnostic marker for several cancers.[8]

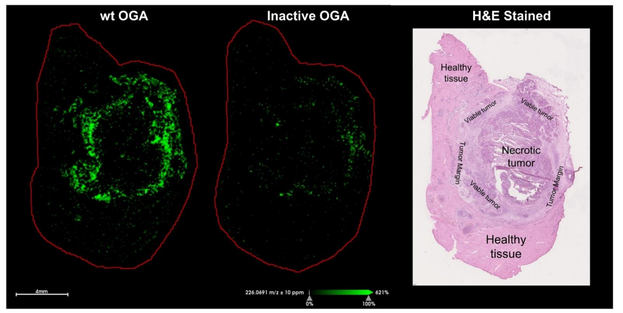

Figure 5. Carnoy's fluid washed tissue sections were treated with wtOGA or inactive OGA, incubated at 30°C with a heating pad to avoid target delovalozation and subsequently sprayed with CHCA for MALDI analysis. A serial section was stained with hematoxylin and eosin to visualize tissue section pathology. The sodium-cationized GlcNAc-oxonium *m/z* 226.0691 – is monitored using SCiLS.

Identified Protein	Protein Best Score	Identified Peptide + O-GlcNAc site	Peptide Byonic Score
Actin, cytoplasmic 1	1428	HQGVMVGMGQKDS[+203.07937]YVG DEAQSKR	531
Calnexin	917	SKPDTSTPPPS[+203.07937]PK	639
Histone H2B	803	GIMNS[+203.07937]FVNDIFER	455
PDZ and LIM domain 5	746	EVVKPVPITSAVS[+203.07937]K	636

Table 1. Summary of O-GlcNAc modified proteins with the identified peptide and O-GlcNAc site. In total, 1916 proteins, 14727 unique peptides, and 23 O-GlcNAc modified PSM's using both HCD/UVPD were identified. Results were gathered via PAGE peptide extraction and separation using nanoLC-MS/MS. An HCD-triggered-UVPD approach was used to characterize O-GlcNAc modified peptides.

Conclusions

- O-GlcNAc was successfully released from peptide standards and tissue sections via spray application of OGA and humidified incubation
- Localization and relative abundance of O-GlcNAc was mapped by MALDI MSI

References

1. McDowell, C. T.; Klamer, Z.; Hall, J.; West, C. A.; Wisniewski, L.; Powers, T. W.; Angel, P. M.; Mehta, A. S.; Lewin, D. N.; Haab, B. B.; Drake, R. R. Imaging Mass Spectrometry and Lectin Analysis of N-Linked Glycans in Carbohydrate Antigen–Defined Pancreatic Cancer Tissues. Molecular & Cellular Proteomics 2021, 20.
2. Angel, P. M.; Mehta, A.; Norris-Caneda, K.; Drake, R. R. MALDI Imaging Mass Spectrometry of N-Glycans and Tryptic Peptides from the Same Formalin-Fixed, Paraffin-Embedded Tissue Section. Methods Mol Biol 2018, 1788, 225–241.
3. Wulff-Fuentes, E.; Berendt, R. R.; Massman, L.; Danner, L.; Malard, F.; Vora, J.; Kahsay, R.; Olivier-Van Stichelen, S. The Human O-GlcNAcome Database and Meta-Analysis. Sci Data 2021, 8 (1), 25.
4. Worth, M.; Li, H.; Jiang, J. Deciphering the Functions of Protein O-GlcNAcylation with Chemistry. ACS Chem. Biol. 2017, 12 (2), 326–335.
5. Ciraku, L.; Esquea, E. M.; Reginato, M. J. O-GlcNAcylation Regulation of Cellular Signaling in Cancer. Cellular Signalling 2022, 90, 110201.
6. Sun, L.; Lv, S.; Song, T. O-GlcNAcylation Links Oncogenic Signals and Cancer Epigenetics. Discov Oncol 2021, 12, 54.
7. Harris GA, Nicklay JJ, Caprioli RM. Localized in situ hydrogel-mediated protein digestion and extraction technique for on-tissue analysis. Anal Chem. 2013 Mar 5;85(5):2717-23.
8. Kobayashi, M.; Nagashio, R.; Jiang, S.-X.; Saito, K.; Tsuchiya, B.; Ryuge, S.; Katono, K.; Nakashima, H.; Fukuda, E.; Goshima, N.; Satoh, Y.; Masuda, N.; Saegusa, M.; Sato, Y. Calnexin Is a Novel Sero-Diagnostic Marker for Lung Cancer. Lung Cancer 2015, 90 (2), 342–345.